Wake deficit-and turbulence simulated with two models compared with inflow measurements on a 2MW turbine in wake conditions

Madsen Aagaard, Helge; Larsen, Gunner Chr.; Larsen, Torben J.; Mikkelsen, R.; Troldborg, Niels

Published in:
Scientific proceedings

Publication date:
2008

Document Version
Publisher's PDF, also known as Version of record

Wake deficit-and turbulence simulated with two models compared with inflow measurements on a 2MW turbine in wake conditions

Helge Aagaard Madsen, Gunner C. Larsen and Torben J. Larsen

Risoe DTU, National Laboratory of Sustainable Energy
Wind Energy Department
Programme for Aeroelastic Design
P.O. Box 49
DK-4000 Roskilde

Robert Mikkelsen and Niels Troldborg

Department of Mechanical Engineering, MEK, Fluid Mechanics Sec.
Nils Koppels Alle, 2800 Lyngby.
Technical University of Denmark, DTU.

helge.aagaard.madsen@risoe.dk
phone +45 46775047

Abstract

Detailed wake characteristics are simulated with two different models; the actuator line (ACL) wake model with turbulent inflow conditions and the engineering Dynamic Wake Meandering (DWM) model. The ACL wake model, based on the EllipSys3D CFD code, simulates all the basic physical phenomena of the wind turbine wake, whereas the DWM model is an engineering code with much less computational demands than the ACL wake model but still modelling the most important physical characteristics of the wake, i.e. the deficit meandering and the added wake turbulence. The simulated results are compared to experimental results from an innovative experimental setup comprising inflow measurements with a five hole pitot tube on a full scale 2 MW turbine operating in wake conditions. Details of wake turbulence characteristics are presented and discussed. The length scale of the added wake turbulence was estimated to 8 m from the ACL results and this is considerable less than the length scale of 33 m of the ambient turbulence. The added wake turbulence only increased the flapwise fatigue loads with 6% in the present case.

1. Introduction

The phenomenon of wake meandering is long known empirically, but has not until recently been treated in a satisfactory manner on the wind turbine load modelling side.

In [1] a consistent, physically based, theory for wake meandering is formulated. Contrary to the traditional wake *load* approach, based on introduction of the concept of effective turbulence originally resulting from the Joule project "Dynamic Loads in Wind farms" [2], the new approach is a *unifying* description in the sense that both turbine *power* and turbine *load* aspects can be treated simultaneously. This feature potentially opens for wind farm topology as well as wind farm control optimization, which is expected to be of crucial economic importance for design and operation of large (offshore) wind farms as well as improving loads predictions for turbines in wake in general.

A key driver/motivation for the formulation of the new wake theory is the recognition that the wake generated intermittent *dynamic loading* of down stream turbines results in both an increased (apparent) turbulence *intensity* and a significantly modified *structure* of the (apparent) turbulence as seen by down stream turbines. We consider both correct turbulence intensity and correct turbulence structure as crucial for realistic load prediction. This is because an increase of the turbulence intensity basically will result in identical *relative* loads increments in all turbine subcomponents, whereas a modified turbulence structure in general will result in significantly different impacts on different turbine components.

In the meandering frame of reference, the *wake* is characterized by a mean wind decrease (i.e. wake deficit) and a significantly modified turbulence field. In a wake

load context, the meandering wake deficit is of primary importance for the increased loading of a turbine operating in a wake and this is the basic mechanism in the DWM model complex presented first time in 2003, [3], [4] and subsequently applied to characterization of extreme loads in wake operation [5].

In the first versions of the DWM model the increased wake turbulence (added wake turbulence) was not included. However, a first attempt to include this in the model was presented in a paper from 2005 [6].

The *turbulence effects*, caused by an upstream located turbine, concern generation of additional small-scale turbulence with characteristic eddy sizes up to approximately one rotor diameter, and include contributions from conventional mechanically generated turbulence, caused by the wake shear, as well as from the blade bound vorticity, consisting mainly of tip and root vortices. The tip vortices will initially take the form of organized coherent flow structures, but later, due to instability phenomenon's, gradually break down and approach the characteristics of conventional isotropic turbulence with a length scale shorter than that of atmospheric turbulence. Wake turbulence is consequently characterized by being both *instationary* (develops with the downstream transportation time) and *inhomogeneous* (vary in general across the wake regime). Typically, the wake turbulence tends to be *more isotropic* and displays *increased turbulence standard deviation* and *reduced turbulence length scale*. The high-frequency part of the spectra will probably follow the inertial sub-range law, but with higher dissipation rate than in the ambient turbulence case. Characterization of wake turbulence and how to model it in the DWM model is the primary subject of the paper.

The characterization of the wake turbulence is mainly based on simulations with a full equation wake model based on the actuator line concept [7], [8] which recently was extended to handle turbulent inflow conditions [9]. This latter extension of the ACL model means that the model now can be run with full realistic inflow conditions and this has developed the model to a strong tool for studying details of the wake flow and for tuning engineering wake models such as the DWM model.

The numerical results are compared to dedicated measurements on a 2MW turbine that was operated in different single wakes from neighboring turbine in the small Tjæreborg wind farm in Jutland, Besides strain-gauges at the blade root, on the shaft and on the tower, the turbine was in a short period in 2002 instrumented with a five hole pitot tube on one of the blades. This instrument gives detailed information about the local inflow to the blade and can therefore be used to characterize the wake flow in a rotating frame of reference. This has the big advantage that simultaneous and instantaneous measurements of wake flow and free flow can be made by measuring in partial wake situations. If further measurements with very low ambient turbulence are selected, the wake meandering will be small and the specific wake turbulence characteristics can be measured without being influenced by apparent turbulence caused by the meandering of the velocity deficit.

2. Model description

This section describes the different models involved in the numerical simulation of the wind turbine wake.

2.1 The ACL model

Navier-Stokes solver

The computations of the global flow field have been carried out using the 3D flow solver EllipSys3D developed by Michelsen [10], [11] and Sørensen [12]. This code solves the discretized incompressible Navier-Stokes equations in general curvilinear coordinates using a block structured finite volume approach. EllipSys3D is formulated in primitive variables (pressure-velocity) in a non-staggered grid arrangement. The pressure correction equation was solved using the SIMPLE algorithm and pressure decoupling is avoided using the Rhie/Chow interpolation technique. The convective terms were discretized using a hybrid scheme combining the third order accurate QUICK (10%) scheme and the fourth order CDS scheme (90%). Large eddy simulation (LES) was used to model the small length scales of turbulence. The resulting equations thus only govern the dynamics of the large scales, while the small scales here were modelled using the so-called mixed scale model [13].

Actuator line model

The wind turbine rotor was simulated using the actuator line model developed by Sørensen and Shen [7]. This model combines a three-dimensional Navier-Stokes solver with a technique in which body forces are distributed radially along lines representing the blades of the wind turbine. Thus, the flow field around and downstream the wind turbine is governed by full three-dimensional Navier-Stokes simulations using LES, whereas the influence of the rotating blades on the flow field is computed by calculating the local angle of attack to determine the local forces from tabulated airfoil data.

Atmospheric boundary layer model

The atmospheric boundary layer is modelled using a technique where body forces applied to the entire computational domain is used to impose a given but arbitrary steady wind shear profile, while free-stream turbulence was modelled by introducing synthetic turbulent velocity fluctuations to the mean flow upstream the rotor.

The method of prescribing a given wind shear profile by imposing body forces was presented by Mikkelsen et al. [8] and is essentially based on the immersed boundary technique. The idea is to conduct an initial computation without the wind turbine included in order to establish the steady force field required to obtain the desired mean wind shear profile. The obtained force field is afterwards stored and kept fixed in the subsequent computation where the wind turbine is included.

The atmospheric inflow turbulence was simulated using a technique [9] where unsteady concentrated body forces, introduced in a plane located 1 rotor radius upstream the upstream rotor, are producing the synthetic turbulent velocity fluctuations. The introduced turbulence field was generated in advance by using the Mann algorithm [14], which simulates homogenous, stationary, Gaussian and anisotropic turbulence with the same spectral characteristics as observed in the atmosphere.

Computational domain and boundary conditions

The computations were conducted in a Cartesian computational mesh with dimensions (x, y, z) = (20R, 24R, 28R), where z is in the flow direction and y is in the vertical direction. The upstream turbine was located 9.5R downstream the inlet and the other turbine was positioned further downstream according to the layout of the wind farm. A high concentration of grid points was distributed equidistantly in the region around and between the two rotors in order to preserve the generated flow structures in the wake. In the equidistant domain a rotor radii was resolved with 30 grid points and outside this region grid points were stretched away towards the outer boundaries. The grid consisted of 144 grid points in respectively the x and y direction and 384 grid points in z-direction. The boundary conditions were the usual inlet and outflow conditions in the main flow direction, no-slip at the ground, far-field velocity at the top and periodic conditions on the sides.

2.2 The DWM model

The Dynamic Wake Meandering (DWM) model complex is based on the combination of three corner stones – 1) modeling of quasi-steady wake deficits, 2) a stochastic model of the down wind wake meandering and 3) added wake turbulence.

The wake meandering part is based on a *fundamental presumption* stating that the transport of wakes in the atmospheric boundary layer can be modeled by considering the wakes to act as *passive tracers* driven by the *large-scale* turbulence structures. Modeling of the meandering process consequently includes considerations of a suitable description of the “carrier” stochastic transport media as well as of a suitable definition of the cut-off frequency defining large-scale turbulence structures in this context.

For the stochastic modeling of wake meandering, we imagine a wake as constituted by a *cascade* of wake deficits, each “emitted” at consecutive time instants in agreement with the passive tracer analogy [1], [19]. We then subsequently describe the propagation of *each* of the “emitted” wake deficits, and the collective description of these thus constitutes the wake meandering model.

Adopting Taylor's hypothesis, the *downstream advection* of these is assumed to be controlled by the mean wind speed of the ambient wind field. With this formulation the wake momentum in the direction of the mean flow is invariant with respect

to the prescribed longitudinal wake displacement. This is a considerable simplification allowing for a straight forward decoupling of the wake along wind deficit profile (and its expansion) and the wake transportation process.

As for the dynamics in the *lateral- and vertical directions*, each considered wake cascade-element is displaced according to the large-scale lateral- and vertical turbulence velocities at the position of the particular wake cascade element at each time instant.

In mathematical terms, the wake deficit dynamics in the lateral direction, *y*, and the vertical direction, *z*, is thus assumed described by the following differential equation system

$$\frac{dy(t,t_0)}{dt} = v_c(y,z,t,t_0) \ , \qquad (1)$$

$$\frac{dz(t,t_0)}{dt} = w_c(y,z,t,t_0) \ , \qquad (2)$$

where v_c and w_c are the spatially dependent large-scale turbulent velocities, and t_0 denotes the time instant at which the considered cascade element is emitted.

The choice of a suitable stochastic turbulence field, that in turn defines the stochastic wake transport process, is not mandatory, but may be guided by the characteristics of the atmospheric turbulence at the site of relevance. These characteristics encompass in principle not only turbulence standard parameters such as turbulence intensity, turbulence length scale and coherence properties, but also features like degree of isotropy, homogeneity of the turbulence, Gaussianity of the turbulence etc..

The meandering mechanism in the DWM model has been successfully verified by correlating DWM predictions with direct full-scale measurements of the instantaneous wake position obtained from LiDAR recordings [18].

Implementation of the DWM model in HAWC2

In the present paper the DWM model is implemented in the aeroelastic code HAWC2 and expanded with some new functionalities. One new thing is that the deficit and the development of the deficit downstream is calculated internally in the code, whereas previous versions of the DWM model used deficits calculated externally by usage of an actuator disc model. Another new feature is the inclusion of added wake turbulence, which represents the turbulence contribution from the upstream turbine, mainly from tip and root vortices. The last new feature is the possibility of having several wake sources, which is especially useful for simulations of turbines in wind farms with more than one neighbouring turbine present.

The DWM model implementation consists of the following 5 steps, where the first 4 are calculated initially:

1. Calculation of the start deficit of the upstream turbine by calculating the induced velocities for a turbine assumed to be identical to the wake turbine but with possible different operational conditions.
2. Expansion of the deficit caused by pressure variation in the near wake region.
3. Developing the deficit as function of downstream distance from the wake generating turbine taking into account the turbulent mixing including the part from ambient turbulence.
4. Wake meandering process of the cascade of deficit centres.
5. Added micro turbulence in the deficit region

Step 1: The wake sources are assumed to consist of turbines with properties identical to the wake loaded turbine. Induced velocities in annular elements are calculated based on traditional BEM theory. Pitch angles and rotational speed are chosen to match the mean operational condition at the selected wind speed.
Step 2: The expansion of the wake caused by the pressure rise in the near wake region (within 2 diameters downstream) is also calculated based on BEM theory. The far wake velocities are reduced to $U_2=U_0(1-2a)$, where the velocities at the rotor is $U_1=U_0(1-a)$. Considering equilibrium of mass flow in an annular stream tube at the turbine and in the far wake is expressed in (3) and (4)

$$\dot{m} = \rho U_0(1-a_i)(r_{t,i+1}^2 - r_{t,i}^2) \qquad (3)$$

$$\dot{m} = \rho U_0(1-2a_i)(r_{w,i+1}^2 - r_{w,i}^2) \qquad (4)$$

leading to an expression of the radius of the next outer element based on the in-

duction and the previous inner element radius in (5).

$$r_{w,i+1} = \sqrt{\frac{1-a_i}{1-2a_i}\left(r_{t,i+1}^2 - r_{t,i}^2\right) + r_{w,i}^2} \qquad (5)$$

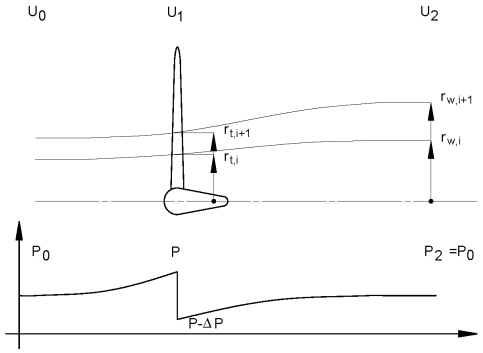

Figure 1: Wake expansion of an annular BEM stream tube due to pressure changes in the near wake region

Step 3: The development of the wake deficit in the far wake field (more than 2 diameters downstream) is except for expansion caused by the local pressure field close to the rotor, mainly affected by turbulent mixing [15], [16], [17], [18]. The implemented model to handle the expansion caused by turbulent mixing is strongly inspired by the work of Ainslie. The turbulent mixing occurring outside the near wake region is described by the Navier-Stokes equations disregarding pressure terms. Further on, the gradients of mean quantities are very much bigger in radial direction (denoted r) than in axial direction (denoted x) which leads to the thin shear layer approximation of the Navier-Stokes equations (6).

$$U\frac{\partial U}{\partial x} + V\frac{\partial U}{\partial r} = -\left(\frac{1}{r}\right)\frac{\partial}{\partial r}\left(r\,\overline{uv}\right) \qquad (6)$$

where U and V denote the mean velocity in the axial- and radial directions, respectively, *u* and *v* denote the respective fluctuating velocity components in these directions, and an upper bar denotes temporal averaging.

Introducing the eddy viscosity concept, the Reynolds stresses are expressed as

$$-\overline{uv} = \upsilon_T \frac{\partial U}{\partial r} \qquad (7)$$

with the eddy viscosity given by

$$\upsilon_T(x) = l_m(x)U_m(x) \qquad (8)$$

where U_m and l_m are suitable velocity- and length scales of the turbulence that in general will vary with the downstream distance *x*, but assumed independent of the radial coordinate. The length- and velocity scales are taken to be proportional to the instantaneous wake half width *b*, and the velocity difference, U_0-U_c, across the shear layer, respectively, where U_0 and U_c denote the ambient velocity and the centre wake velocity. Introducing (7) and (8) into (6) the governing equations are reformulated as

$$U\frac{\partial U}{\partial x} + V\frac{\partial U}{\partial r} = \left(\frac{\upsilon_T}{r}\right)\frac{\partial}{\partial r}\left(r\frac{\partial U}{\partial r}\right) \qquad (9)$$

with

$$\upsilon_T = k_2 b\left(U_0 - U_c\right) + \upsilon_{TA} \qquad (10)$$

where k_2 is an empirical constant for the flow field. k_2=0.002 seems to give results comparable to actuator disc results [18]. υ_{TA} is a viscosity term depending on the ambient turbulence level

$$\upsilon_{TA} = k_1 Ti \qquad (11)$$

where k_1 is another empirical constant and *Ti* is the turbulence intensity of the ambient turbulence.

In addition to the momentum equation (6) the flow must fulfil the continuity equation given by

$$\frac{1}{r}\frac{\partial}{\partial r}\left(rV\right) + \frac{\partial U}{\partial x} = 0 \qquad (12)$$

The flow problem defined by (9) and (12) is solved using a finite difference scheme.

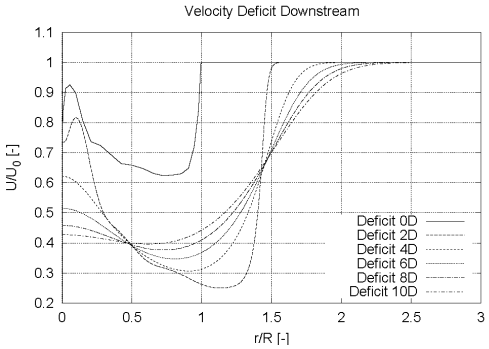

Figure 2: Final deficit in selected downstream distances including pressure expansion from 0D to 2D and turbulent mixing (using k_2=0.002) further downstream.

Step 4: The turbulence field chosen as the stochastic transport media generating the wake meandering is the Mann turbulence model [14], [19], since this turbulence field is fully correlated between *u*, *v* and *w*, formulated in cartesian coordinates and enables unequal grid resolution and size in the three directions, see Figure 3. A

course grid resolution is chosen in the in-plane direction since this first of all enables an effective cut-off frequency filtering neglecting all eddies with a size less than the rotor, secondly to enable very large spatial dimensions of the box which is especially important if several wake sources are considered. A special feature when using several upstream wake sources in the same turbulence field is that if a wake passes the centre of the next turbine, the two wakes will remain together for the rest of the transport since they meet the same turbulence. The grid resolution in the *u*-direction is chosen with a finer resolution in order to get a smooth continuous variation in deficit centre positions. It is important that the grid point velocities represent the mean value of a grid cube in order to provide a correct spatial filtering.

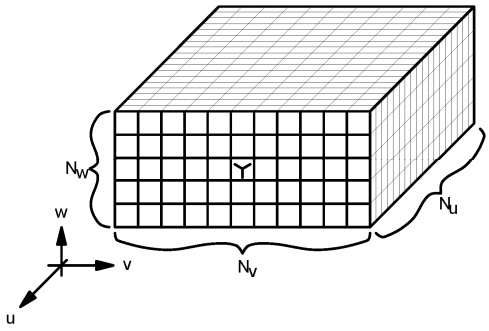

Figure 3: Mann turbulence box layout for the meander turbulence. A course grid resolution (size of 1 rotor diameter) is seen in the in-plane *v*,*w* direction whereas the resolution in the u-direction is chosen to be fine.

Step 5: The turbulence created by the upstream turbine is modelled as a separate Mann turbulence field with a short length scale and a ratio between variance of the *u*, *v* and *w* component of 1.0 corresponding to isotropic turbulence. The resolution of the box is high (128x128 points) in the in-plane direction covering 1 rotor diameter so small eddies can be resolved reasonably. The box length in the *u*-direction consists of 128 points covering 2.5 rotor diameters. Turbulence is reused when points outside the box are requested. The *v*,*w* centre position of this turbulence box follows the centre position of the individual wake deficits. The turbulence is scaled based on the deficit depth and gradient according to (7). Two empirical factors k_{m1} and k_{m2} are inserted to schedule the gain of the two different contributions

$$k_{mt}(r) = \left|1 - U_{def}(r)\right| k_{m1} + \left|\frac{\partial U_{def}(r)}{\partial r}\right| k_{m2} \qquad (13)$$

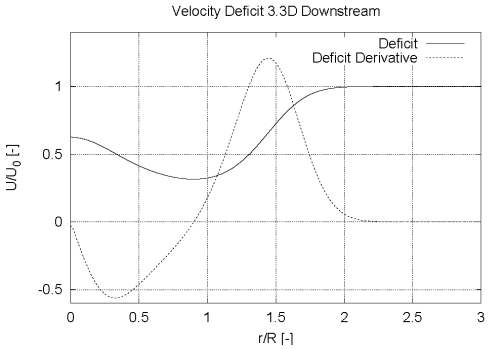

Figure 4: Deficit and derivative used for micro turbulence scaling.

The influence of added wake turbulence can be seen in Figure 5 where small ripples in the angle of attack can be seen when the blade enters a wake load situation. These ripples contribute to small load cycles in the blade loading.

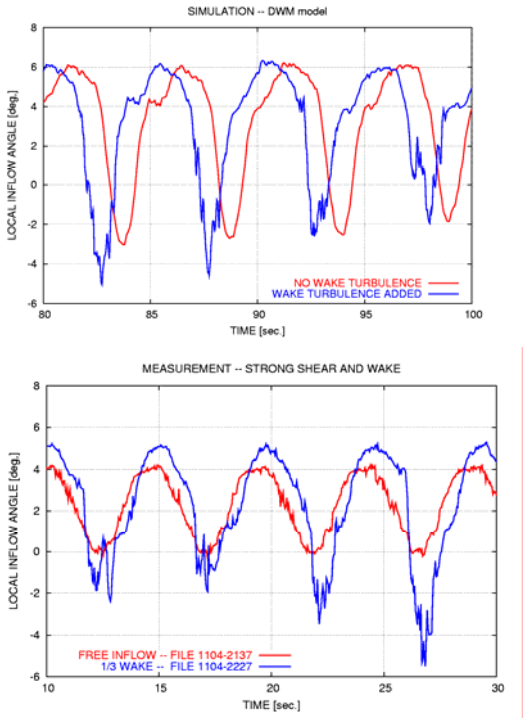

Figure 5: Added wake turbulence causes small ripples in angle of attack when the blade is in the wake loaded area. Top: simulation, bottom: measurements.

3. Full scale experiment

Selected characteristics of the numerical predictions, described in Section 2, are compared with full-scale experimental data obtained from a 2MW wake operating turbine at the Tjaereborg wind farm in Denmark. The rotor diameter of the turbine is 80 m.

The selected characteristics encompass *wake flow field characteristics*, as measured directly in the rotor plane of the wake operating turbine, and induced *structural response characteristics* in the form of blade root moments.

The blade root moments are established by standard strain-gauge recordings, whereas the flow field observations are based on an innovative experimental setup [20] using a five hole pitot tube mounted at the blade leading edge in radius 24 m, Figure 6.

From the five hole pitot tube measurements of the *local inflow angle* in the plane perpendicular to the blade span can be derived and likewise the *local, relative velocity*. Due to the geometrical conditions for the local inflow velocity vector, the relative velocity signal will mainly show the characteristics of the two lateral turbulence components whereas the local inflow angle mainly contain the characteristics of the streamwise turbulence component.

The measured inflow angle was corrected for upwash from the bound circulation on the blade section at the pitot tube whereas no corrections were applied to the measured relative velocity.

As the focus of the present analysis is characteristics of the wake turbulence the data base was searched for inflow conditions with low ambient turbulence as this is expected to give low meandering of the wake. A few data files with such conditions (turbulence intensity around 3%) were found and three 10 min. data files measured within one hour were selected as they contained both free inflow and wake conditions for an upstream turbine in a distance of 3.5 D. Unfortunately, meteorological conditions with low ambient turbulence are often associated with a strong wind shear and a change of wind direction as function of height. This is also the case for the three selected data files but the inflow conditions in the models were adapted to give an optimal correlation between simulated and measured local inflow angle, local relative velocity and flapwise moment, binned on azimuth. The wind shear was modelled with an exponential curve with an exponent of 0.7 and a yaw error of 15 degree was applied. The relative velocity binned on azimuth provides an excellent basis for adjusting the yaw error to the measured data.

Figure 6: The five hole pitot tube mounted on the leading edge of the blade. (The plate mounted on the blade is used for measurement of the angle of the pitot tube relative to the tip pitch).

4. Results

The simulation results are ordered in two parts. Firstly, the DWM and ACL results are compared and different parameters in the DWM model are tuned on basis of this comparison. In this way this section also contains results for discussions of the wake turbulence characteristics as e.g. the turbulence length scale.

In the second part of the results section, the DVM model is run for the specific wake conditions in the three 10 min. experimental data files mentioned above. In these simulations the DWM model is run with the parameters found in the comparison with the ACL model

In all the simulations the strong wind shear as seen in the measurements are applied. However, only the DWM model results are directly compared with the measurements because the experimental conditions were complicated by the wake occurring on the lower part of the rotor. In the ACL model this could potentially give problems with interaction with the ground surface.

4.1 Tuning of parameters in the DWM model

4.1.1 No ambient turbulence

The first load case compared is simulations with the ACL and the DWM with no surrounding turbulence and an offset in turbine position horizontally leading to a 1/3 wake loading. The downstream turbine is further yawed with 15deg since these conditions fits reasonably to a measurement case used in later comparisons. The only variations in wind speed affecting the downwind turbine is the deficit loading 1/3 on the rotor and the wake turbulence from the upstream turbine.

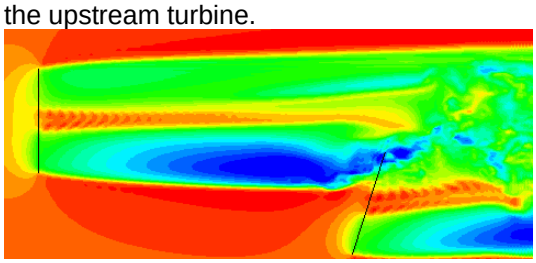

a)

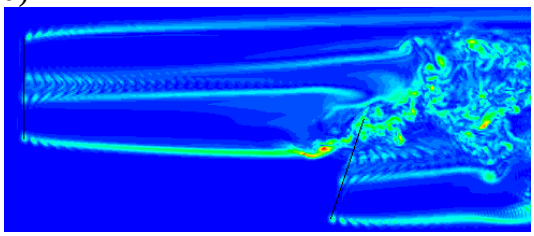

b)

Figure 7: Visualization of flow field in a horizontal plane located in hub height. The rotors are indicated as black lines and the inflow is laminar; a) Stream-wise velocity; b) vorticity

Contour plot of axial velocity and vorticity computed for this case with the ACL model is shown in Figure 7. As seen the wake of the upstream turbine is characterized by significant asymmetry due to the non-uniform rotor loading caused by a combination of the turbine tilt angle and the strong shear. Furthermore, the figures reveal a considerable inhomogeneous turbulence field inside the wake. It is also seen in Figure 7 that the wake profile changes immediately before the downwind turbine. A horizontal shift occurs. In order to make comparable results to the DWM model a horizontal offset of 1.9R is assumed in the DWM simulation where the offset is 1.6R in the ACL simulations.

The standard deviation of the angle of attack, relative velocity and flapwise bending moment in Figure 9 was used to tune the empirical constants k_{m1} and k_{m2} for the added wake turbulence. The rainflow counted load histogram in Figure 9 was likewise used to determine the correct length scale of the added wake turbulence. A good agreement between the two models is seen with k_{m1}=0.6, k_{m2}=0.25 and a length scale of the wake turbulence of 8m (IEC definition of length scale).

The time length of the ACL simulations is about 3 min. and it can bee seen from the narrow band of the st. dev. of the different parameters that there is no indication of a meandering of the deficit.

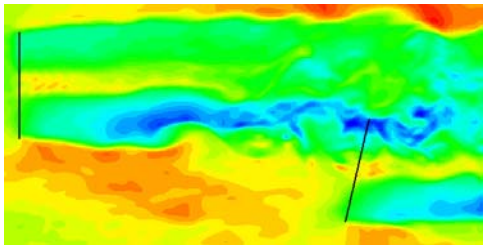

a)

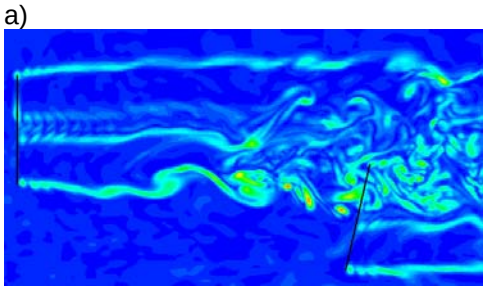

b)

Figure 8: Visualization of flow field in a horizontal plane located in hub height. The rotors are indicated as black lines and the inflow is turbulent; a) Stream-wise velocity; b) vorticity

4.1.2 Influence of ambient turbulence

In the next simulation case, 3% turbulence is added to the inflow. This value was selected to fit the measurements although the case will not directly be used for comparison of the simulations with measurements as the 1/3 wake condition is still specified in the horizontal plane. However, the analysis of the turbulence used for the ACL model showed afterwards that the level was about 4%. The influence of the ambient turbulence is clearly seen in the contour plot of the velocity *u* and vorticity, computed with the ACL model, Figure 8. The flow field is now much more scattered when compared with the flow field in Figure 7.

With added turbulence the wake, turbulence characteristics become much more complex than in the case with laminar inflow. In the DWM model the 3% turbulence is also specified for the wake meandering turbulence box and a meandering trace in vertical and horizontal direction is computed causing the velocity deficit to change position as function of time. This will give variations in the inflow angle but almost no influence of the relative velocity [6]. The development of the velocity deficit from the upstream to the downstream turbine is also influenced by the ambient turbulence as specified by (11) where the constant k_1 has to be determined. As the added turbulence in the DWM model depends on the characteristics of the actual deficit at the wake operating turbine, its characteristics are indirectly influenced by the ambient turbulence.

To illustrate the influence of k_1, simulation results with the DWM model for k_1=0 is shown in comparison with results for k_1=0.001 which was the value selected to give the best fit. With k_1=0 there is only a limited change of the velocity deficit as only the turbulence mixing from the radial gradients of the deficit itself is present. This gives a high st. dev. on the local inflow angle and the flapwise moment as can be seen in Figure 10 because the depth of the deficit and the gradients are only slightly changed and thus the added wake turbulence will be high.

With a value of k_1=0.001 the average level of the st. dev. of local inflow angle and the flapwise moment, respectively fits reasonably whereas the shape of the curves differ somewhat more. It should also be noted that the level of relative velocity simulated with the DWM model decreases slightly. This is because there is almost no contribution to this velocity component from the meandering but only from the added wake turbulence which generally will decrease for increasing downstream distance. However, the ACL results show some increase for the relative velocity meaning increase in the two lateral turbulence components.

The azimuth interval with increased st. dev. on the parameters has increased compared with the zero ambient turbulence case but still only about half of the azimuth interval is influenced.

The Rainflow counting of cycles of the flapwise moment shows in general good agreement between the two models, Figure [9] Figure 10.

4.2 Comparison of the DWM model with measurements

With the constants in the DWM model tuned to the results of the ACL model, simulations with the DWM model were run for the three different wake conditions in the measurement. As mentioned, the wake condition occurred on the lower part of the rotor centered almost around an azimuth of 180 deg as seen in Figure 11. Free inflow, 1/3 and 2/3 wake conditions were simulated (1/3 and 2/3 is an approximate characterization of how much of the swept are is covered of the velocity deficit from the upstream turbine). In these simulations the turbine model was with normal flexibility of the turbine structure whereas a stiff turbine model was used in the comparisons of the DWM and ACL model.

The same comparisons as presented earlier in the paper were made for this case and the results are depicted in Figure 11. Overall, there is a good correlation between the DWM results and the measurement as concerns the st. dev. of the different parameters binned on azimuth. As an example the double peeks in the st. dev. of the flapwise moment is seen both in the simulations and in the measurements. The biggest difference between the DWM model and the measurements is on the Rainflow counting results of the flapwise moment, Figure 11. The 2/3 wake condition causes considerably higher fatigue loads in the simulations compared with the measurements. The difference seems to be caused by a somewhat lower deficit in the experiment than computed with the DWM model. For the smaller cycles it seems that the added wake turbulence improves the correlation with experiment. However, the increase in fatigue caused by the added wake turbulence was only about 6% for the present case.

Finally, the simulated and measured PSD spectra of the relative velocity and the flapwise moment are compared in Figure 12. The general correlation between the simulated and measured spectra is good. One simulation was made without added wake turbulence and the simulated spectrum of the relative velocity then differs considerably from the measured.

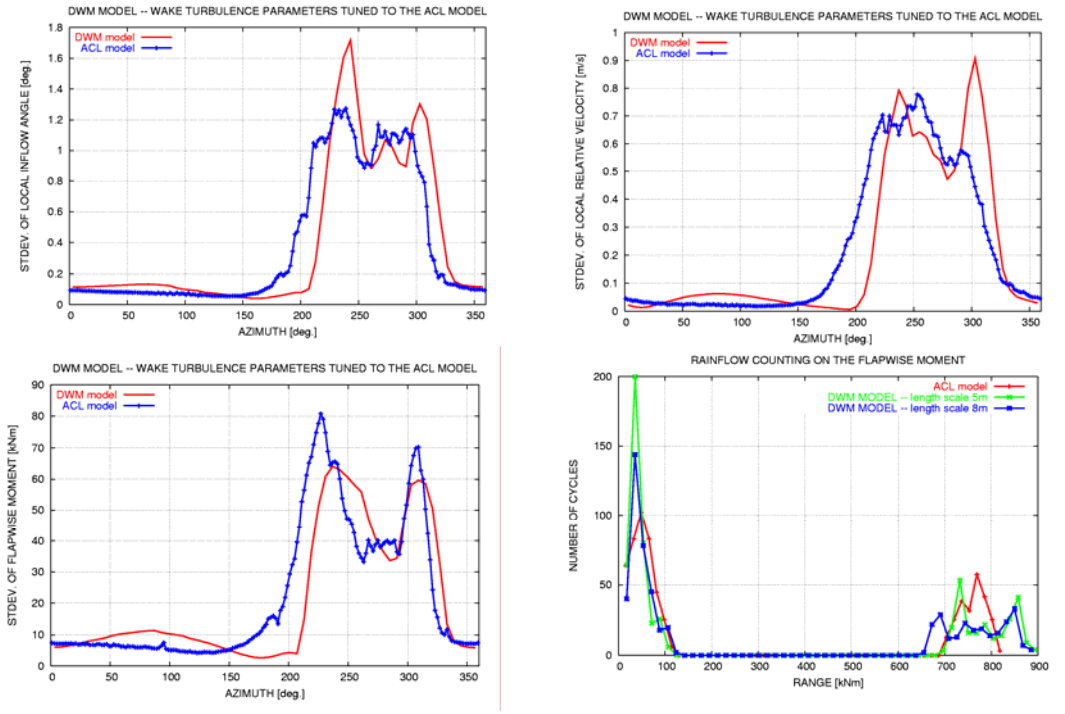

Figure 9: Comparison of angle of attack and relative velocity in radius 24m and flapwise bending moment at root with 1/3 wake loading between the ACL and the DWM models. No ambient turbulence present.

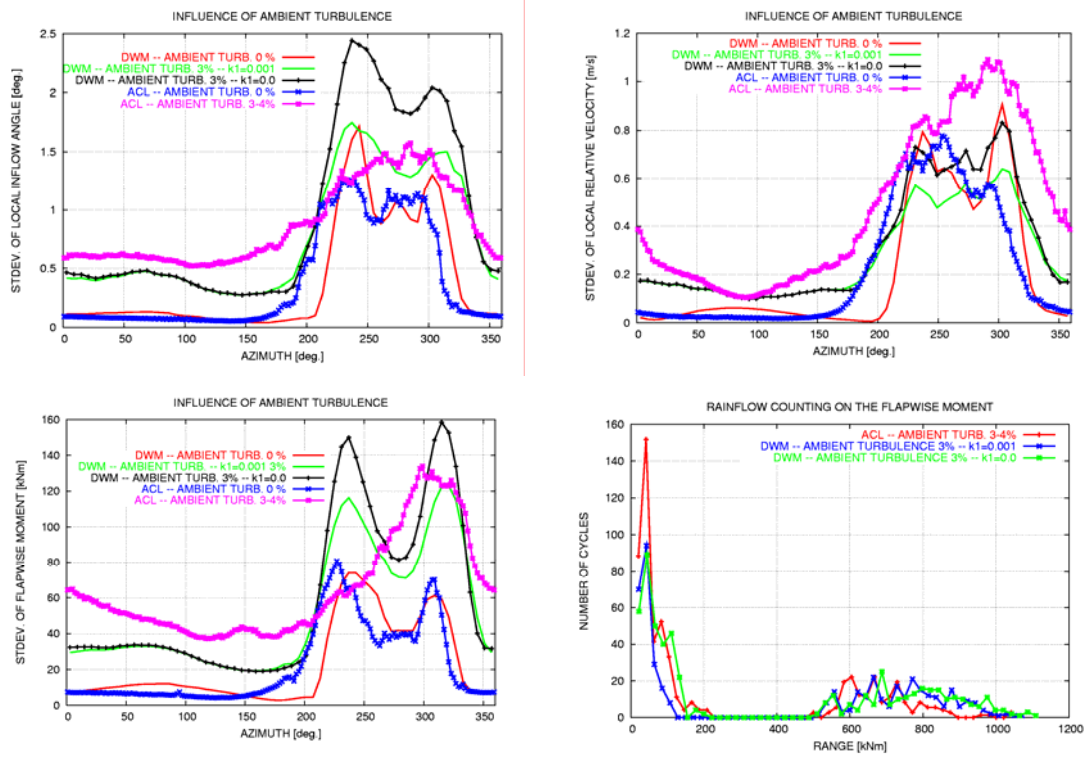

Figure 10: Comparison of angle of attack and relative velocity in radius 24m and flapwise bending moment at root with 1/3 wake loading between the ACL and the DWM models. Influence of ambient turbulence and of the k_1 parameter in the BLE model.

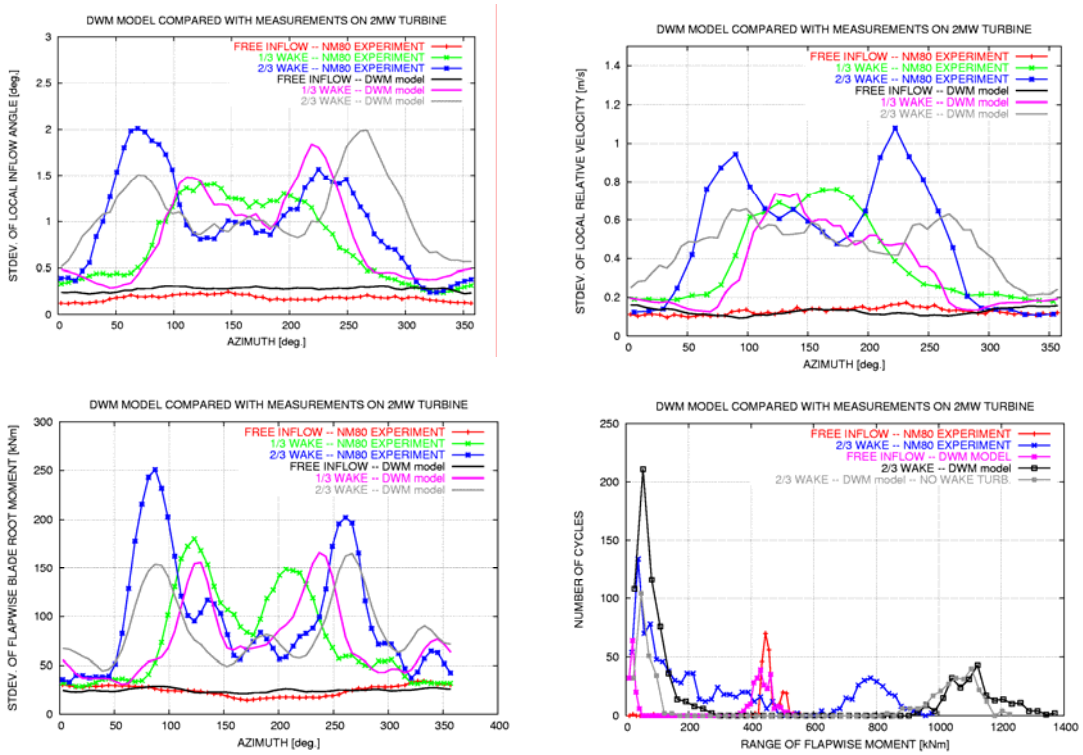

Figure 11: Comparison of std. of the local inflow angle, local relative velocity and flapwise moment, simulated with the DWM model and compared with experiment. Figure in bottom, right corner shows rainflow counting results on the flapwise moment.

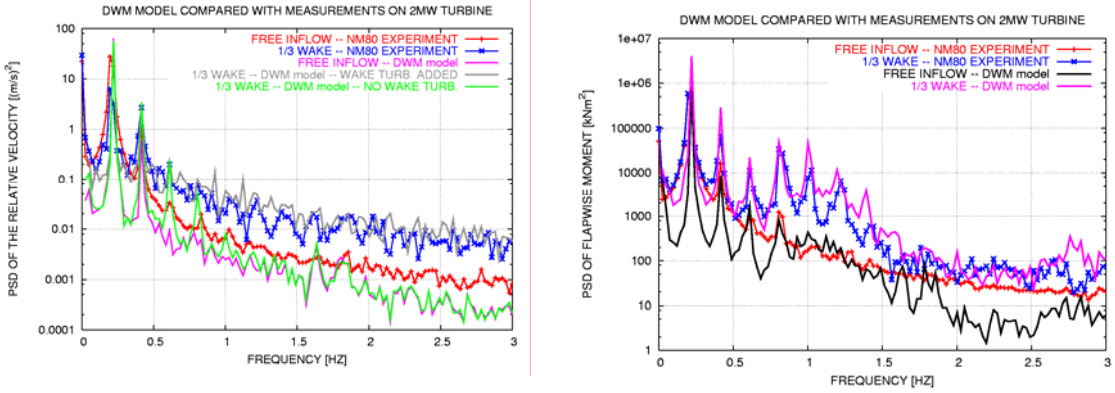

Figure 12: PSD spectra of the relative velocity and the flapwise blade root moment for free inflow and for 1/3 wake operation computed with the DWM model and compared with experiment.

5. Summary

The DWM model has been further developed and is now fully integrated in the aeroelastic model HAWC2. The development of the velocity deficits is performed with a boundary equation model. Tuning of model parameters in the DWM model has been performed by comparing results with the ACL model which now can be run with turbulent inflow. On basis of the ACL results, the wake turbulence has been characterized and the parameters in the DWM model were tuned.

Using a length scale of 8 m (10% of rotor diameter) for the wake turbulence in the DWM model and further assuming isotropy gave a good correlation when comparing with the ACL model results. The added wake turbulence increased the fatigue load of the flapwise blade root moment with 6% for the present case, indicating that added wake turbulence is not the major cause of increased loading in wakes. Finally, the DWM model results were compared with experimental data from a

2MW wind turbine and in general a good agreement was found.

6. References

[1] Larsen, G.C., Madsen, H. Aa., Thomsen, K. and Larsen, T.J.. Wake meandering - a pragmatic approach, which has been accepted for publication in Wind Energy.

[2] Tindal, A.J. "Dynamic Loads in Wind Farms", Final Report, CEC Project JOUR-0084-C, 1993.

[3] Madsen, H.A., Thomsen, K. and Larsen, G.C. "A New method for Prediction of Detailed Wake Loads". Proceedings of IEA Joint Action of Wind Turbines 16th Symposium held in Boulder, USA, May 2003 at NREL, edited by Sven-Erik Thor. pp. 171-188.

[4] Thomsen, K., Madsen, H.A,, Larsen, G.C. "A New method can predict detailed response for turbines in wind farms". Fact sheet AED-RB-16(EN), Risø National Laboratory, Roskilde 2003.

[5] Thomsen, K., Madsen, H.A. "A New Simulation Method for Turbine in Wakes – Applied to Extreme Response during Operation". Wind Energy 2005, 8, pp. 35-47.

[6] Madsen, H.A., Larsen, G.C., and Thomsen, K. (2005). "Wake flow characteristics in low ambient turbulence conditions". In: proceedings of Copenhagen Offshore Wind 2005.

[7] Sørensen, J.N. and Shen, W.Z. "Computation of Wind Turbine Wakes using Combined Navier-Stokes/Actuator-line Methodology". Proc. European Wind Energy Conference EWEC '99, 56-159, Nice, 1999

[8] Mikkelsen, R., Sørensen, J.N. and Troldborg, N. "Prescribed wind shear modelling combined with the actuator line technique". Conf. Proc. EWEC, 2007, Milano, Italy.

[9] Troldborg, N., Sørensen, J.N. and Mikkelsen, R. "Actuator Line Simulation of Wake of Wind Turbine Operating in Turbulent Inflow". 2nd EWEA conf. on the Science of Making Torque from Wind, 2007, Lyngby, Denmark.

[10] Michelsen, J.A., "Basis3D – a Platform for Development of Multiblock PDE Solvers", Report AFM 92-05, Dept. of Fluid Mechanics, Technical University of Denmark, DTU, 1994.

[11] Michelsen, J.A., "Block Structured Multigrid Solution of 2D and 3D elliptic PDE's", Report AFM 94-06, Dept. of Fluid Mechanics, Technical University of Denmark, DTU, 1994.

[12] Sørensen, N.N., "General Purpose Flow Solver Applied to Flow over Hills", PhD Dissertation, Risø-R-827(EN), Risø National Laboratory, Roskilde, Denmark, 1995.

[13] Saugaut, P., "Large Eddy Simulation for Incompressible Flows – An Introduction", Springer, 2005

[14] Mann J. Wind field simulation. Prob. Engng. Mech. Vol. 13, No. 4, pp. 269-282, 1998.

[15] Ainslie, J.F. "Development of an eddy viscosity model for wind turbine wakes". In: Proceedings of the BWEA conference 1985, pp.61-66

[16] Ainslie, J.F. "Wake modeling and the prediction of turbulence properties". In Proceedings of th 8th British Wind Energy Association Conference, Cambridge 19-21 March. pp. 115-120

[17] Ainslie, J.F. "Calculating the flow field in the wake of wind turbines". Journal of Wind Engineering and Industrial Aerodynamics, 27, pp. 213-224

[18] Larsen G.C, Madsen, H.A., Bingöl F., Mann J., Ott S., Sørensen J.N., Okulov V., Troldborg N., Nielsen M., Thomsen K., Larsen T.J., Mikkelsen R. "Dynamic wake modeling". Risø-R-1607(en). Risoe National laboratory – Technical University of Denmark. 2007.

[19] Mann, J. (1994). "The Spatial Structure of Neutral Atmospheric Surface-Layer Turbulence". J. of Fluid Mech., **273**, 141-168.

[20] Madsen, H.Aa., Thomsen, K. and Petersen, S.M. (2003). "Wind Turbine Wake Data from Inflow Measurements using a Five Hole Pitot Tube on a NM80 Wind Turbine Rotor in the Tjæreborg Wind Farm". Risø-I-2108(EN).